Quantum magnetic oscillations and angle-resolved photoemission from impurity bands in cuprate superconductors

A. S. Alexandrov[*]

Instituto de Fisica Gleb Wataghin/DFA, Universidade Estadual de Campinas-UNICAMP 13083-859, Brasil

(Received 31 January 2012; revised manuscript received 10 February 2012; published 7 March 2012)

Present-day angle-resolved photoemission spectroscopy (ARPES) has offered a tremendous advance in the understanding of electron energy spectra in cuprate superconductors and some related compounds. However, in high magnetic field, magnetic quantum oscillations at low temperatures indicate the existence of small electron (hole) Fermi pockets seemingly missing in ARPES of hole (electron) doped cuprates. Here ARPES and quantum oscillations are reconciled in the framework of an impurity band in the charge-transfer Mott-Hubbard insulator.

ARPES of cuprate superconductors[1] proved to be particularly instrumental in modeling the electron energy spectrum of these charge-transfer Mott-Hubbard insulators showing that below optimal doping the single-particle Fermi surface is reduced to four disconnected peculiar-shaped spots. While on the overdoped side of the phase diagram a large Fermi surface is expected and observed,[2] a few holes doped into the insulator would naturally give rise to four hole "nodal Fermi pockets" with a small area proportional to the doping on the underdoped side of the phase diagram. Another possibility is a truncation of the large hole Fermi surface giving rise to four "nodal Fermi arcs" due to a highly anisotropic quasiparticle lifetime and/or a d-wave-like pseudogap. Remarkably, magnetic quantum oscillations (MQO) in kinetic and magnetic response functions of oxygen-ordered ortho-II YBa$_2$Cu$_3$O$_{6.5}$ (YBCO6.5) and of some other cuprates[3] revealed small *electron* Fermi pockets rather than hole pockets or arcs, seemingly in disagreement with ARPES results.[1]

A number of Fermi surface reconstructions[4] and non-Fermi-liquid models, including our modulated vortex lattice scenario,[5] have attempted to account for the nature of these unusually slow MQO. Further careful experiments have found the Zeeman splitting in MQO, which separates spin-up and spin-down contributions, indicating that electrons in cuprates behave as nearly free spins, which rules out most of the reconstruction and non-Fermi liquid scenarios.[6] This observation, as well as excellent fits of MQO data with field-independent oscillation frequencies, supports the view[3] that MQO are a signature of the true zero-field normal state. This view is also supported by the observation of similar slow oscillations in electron-doped cuprates Nd$_{2-x}$Ce$_x$CuO$_4$ (NCCO),[7] where due to their lower critical fields, the normal state is reliably accessed for any doping level. In contrast with the *electron* pockets in *hole* doped cuprates, MQO reveal small *hole* pockets around a certain doping level $x \approx 0.165$ in *electron* doped cuprates.[8]

Until recently these two different measurement techniques, ARPES and MQO, were carried out on different materials. Aiming to resolve the outlined puzzle, Hossain *et al.*[9] were able to control the surface doping and follow the evolution of ARPES from the overdoped to the underdoped regime through an *in situ* deposition of potassium atoms on cleaved YBCO. Reference 9 did not find any sign of the electron pockets in the ARPES data from underdoped YBCO, nor any sign of extra

zone folding due to the kind of density wave instabilities that might give rise to such a Fermi surface reconstruction. Hossain *et al.* argued that if any pocket had to be postulated on the basis of their ARPES data, the most obvious possibility would be that the Fermi arcs are in fact nodal Fermi pockets. However, these are hole, not electron, pockets.

Apparently without a detailed microscopic theory, both ARPES and MQO data remain a mystery. Here I reconcile these two rather precise techniques by introducing an impurity band in the doped charge-transfer Mott-Hubbard insulator. Small electron (hole) pockets in the impurity band account for MQO observed in hole (electron) doped cuprates,[3,7] and for the "half-moon" spots in ARPES.[9]

Cuprate superconductors are strongly correlated electron systems where the *ab initio* local-density approximation (LDA) fails especially in the undoped regime. Fortunately, adding the on-site Coulomb repulsion U to the LDA analysis within the LDA + U algorithm[10] or using LDA plus the tight-binding (cluster) approximation (LDA + GTB algorithm[11]), one can reproduce the correct magnetic ground state and the charge-transfer gap in parent insulators such as La$_2$CuO$_4$ (LCO). The latter and some other schemes[12] for the electronic structure found the charge-transfer gap also in the paramagnetic state of cuprates, pointing to a persistent Mott physics also at finite doping.[13] While ARPES electronic structures of the overdoped cuprates are found in agreement with the density functional theory and Fermi-liquid-like descriptions, there is a clear departure from Fermi-liquid behavior and a more rapid than expected crossover to Mott physics already at optimum doping in the underdoped region.[14]

Different from the reconstruction models proposed so far, I suggest that YBCO6.5 is the Mott-Hubbard insulator where the Fermi level is pinned within the charge-transfer gap as in its parent insulator YBCO6.0.[4] Our assumption is supported by experiments with ultrathin insulating La$_2$CuO$_4$ and doped superconducting La$_{2-x}$Sr$_x$CuO$_4$ (LSCO) layers[15] and by earlier optical spectroscopies of YBCO[16,17] indicating that doped electronic states appear within the charge-transfer gap. These states, localized in band-tails by disorder, readily account for sharp "quasiparticle" peaks and a rapid loss of their intensities in some directions of the Brillouin zone observed in ARPES of lightly doped LSCO.[18] Loss of quasiparticle integrity in underdoped YBa$_2$Cu$_3$O$_{6+x}$ has been experimentally observed by means of ARPES and an *in situ* doping technique,[14] fully
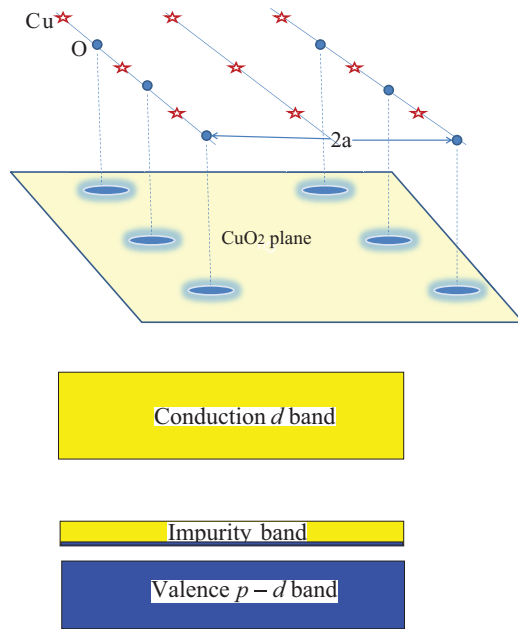
FIG. 1. (Color online) The ortho-II phase of $YBa_2Cu_3O_{6.5}$ is characterized by a periodic alternation of empty Cu and filled Cu-O b-axis chains doubling the unit cell in the a direction. Extra oxygen in the full chains gives rise to an attractive potential for the holes (upper panel) creating a coherent band inside the charge-transfer gap of the Mott-Hubbard insulator (lower panel).

compatible with our assumption. The same band-tail model explains two energy scales, their temperature and doping dependence, and the asymmetry and inhomogeneity of tunneling spectra of cuprate superconductors.[19] The superconductivity is supported by the preformed real-space pairs (bipolarons), and the pseudogap is half of the bipolaron binding energy in this model. Magnetic fields used in MQO experiments could hardly destroy bipolarons and their condensed state[5] so that conventional Fermi-liquid quasiparticles in the band tails coexist with the bipolaronic (d-wave) condensate in agreement with the recent specific heat study.[20] Pinning the Fermi level within the impurity band tail is also compatible with the insulatinglike low-temperature normal state resistivity and many other kinetic properties of underdoped cuprates.[18,21,22] With increasing doping, the bipolaron binding energy decreases due to screening effects, so that the Fermi level enters the valence band at overdoping.

In the LDA picture, the extra oxygen in the full chains of $YBa_2Cu_3O_{6.5}$, Fig. 1, splits the planar CuO_2 metallic band in two with a gap opening at the new Brillouin zone boundary $k_x = \pm\pi/2a$, estimated from local-density approximation calculations between 120 and 160 meV.[23] Quite a different band structure emerges in the charge-transfer insulator. Our key point is that, at variance with other doping levels, 0.5 (per unit cell) extra oxygen creates a coherent band within the charge-transfer gap rather than the localized band tail, since YBCO6.5 is perfectly ordered, as seen in Fig. 1. As shown below, this coherent band accounts for the observed quantum oscillations, and its spectral function combined with the matrix elements also explains ARPES. To gain insight into the coherent "impurity" band dispersion of YBCO6.5, we

employ the LDA + U band structure of the parent insulator YBCO6.0.[4] In such a framework, the CuO_2 in-plane states are found about 0.5 eV below the Fermi level, and the first electron-removal (i.e., valence) state has a BaO-Cu chain character (see Fig. 5 in Ref. 4). This valence band has its maximum at the Γ point of the Brillouin zone. Spin fluctuations and significant electron-phonon interactions[21] could push the in-plane states closer to the Fermi energy, thus back into the first ionization energy range, due to polaronic level shifts missing in the LDA + U band structures. The edge of the upper in-plane band is also found at the Γ point in YBCO6.0,[4] therefore which particular orbitals form the valence band is not an issue in our further analysis. In any case, we are dealing with quasi-two-dimensional carriers.

A single extra oxygen ion in the chain creates the Coulomb attractive potential for a hole, about $-2e^2/\epsilon\rho$, at a large enough distance ρ from the ion. Solving the 2D Coulomb problem in the effective mass (m) approximation yields an estimate of the localized state ionization energy, $E_{im} = 8me^4/\hbar^2\epsilon^2$. E_{im} is about 87 meV with $m = 2m_e$ measured in MQO experiments[3] and with $\epsilon = \sqrt{\epsilon_{ab}\epsilon_c}$, where $\epsilon_{ab} = 500$ (Ref. 24) and $\epsilon_c = 10$ (Ref. 25) are the in-plane and c-axis dielectric permittivities, respectively, measured in the insulating YBCO single crystals. This energy is much lower than the charge-transfer gap, which is about 1 eV,[4] so that the bound state is rather shallow. The size of the bound-state wave function, $f_{im}(\rho) \propto \exp(-\rho/a_{im})$, is comparable to the lattice constant, $a_{im} = \hbar^2\epsilon/4me^2 \approx 0.4$ nm.

Excess oxygen ions in YBCO6.5 give rise to a potential $V(\vec{\rho})$ (see Fig. 1) periodic in a plane $\vec{\rho} \equiv \{x, y\}$. It is "gentle" in the outlined sense due to the high polarizability, $\epsilon \gg 1$, of perovskites, so that the valence-band states of the parent insulator are mainly involved. Hence the impurity-band wave function $\psi(\mathbf{r})$ can be expanded in a complete set of the orthogonal valence-band Wannier functions $w(\mathbf{r})$, which account for most of the correlations.[11] These functions are atomiclike with their extension, a_0 smaller than the lattice constant a. Thus $\psi(\mathbf{r}) = \sum_{\mathbf{m}} F(\mathbf{m})w(\mathbf{r} - \mathbf{m})$, where the envelope function $F(\mathbf{m})$ satisfies the following differential equation[26]

$$[E(-i\vec{\nabla}_\rho) + V(\vec{\rho})]F(\vec{\rho}) = E_{im}F(\vec{\rho}). \quad (1)$$

Here $E(\mathbf{p})$ is the LDA + U dispersion of the 2D valence band.[4] The eigenstates of Eq. (1) can be expanded as

$$F_{\mathbf{k}}(\vec{\rho}) = \frac{1}{\sqrt{N_{im}}} \sum_{\mathbf{n}} e^{i\mathbf{k}\cdot\mathbf{n}} f(\vec{\rho} - \mathbf{n}), \quad (2)$$

since the potential $V(\vec{\rho})$ is periodic. Here $\mathbf{k}$ is the quasimomentum in the reduced 2D Brillouin zone, $(-\pi/2a < k_x < \pi/2a, -\pi/a < k_y < \pi/a)$, $f(\vec{\rho} - \mathbf{n})$ are the orthogonal impurity-band Wannier orbitals built of the bound-state wave function $f_{im}(\vec{\rho})$, and $\mathbf{n}$ are 2D position vectors of excess-oxygen ions N_{im} or their projections in the plane (see Fig. 1). Then the impurity-band dispersion is found as

$$E_{im}(\mathbf{k}) = -\sum_{\mathbf{n}} e^{i\mathbf{k}\cdot\mathbf{n}} t(\mathbf{n}), \quad (3)$$

where $t(\mathbf{n}) = -\int d\vec{\rho} f(\vec{\rho} + \mathbf{n})[E(-i\vec{\nabla}_\rho) + V(\vec{\rho})]f(\vec{\rho})$ are the impurity-band hopping integrals, which are positive for the attractive $V(\vec{\rho})$. It should be noted that the impurity-band
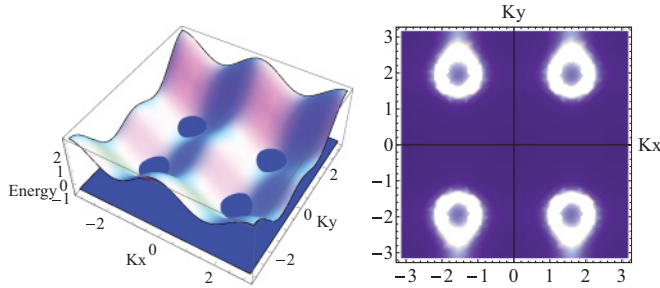
FIG. 2. (Color online) The impurity-band energy dispersion in $YBa_2Cu_3O_{6.5}$ with four small electron pockets at the reduced Brillouin zone boundary (dark oval spots) as described by Eq. (4) with $t' = 0.7t$ and the Fermi level $\mu = -2.5t$ (Energy is measured in $2t$ and $a = 1$, left panel). Right panel: The momentum-distribution map of the impurity-band spectral function at the Fermi surface with the same parameters and $\gamma = 0.04t$.
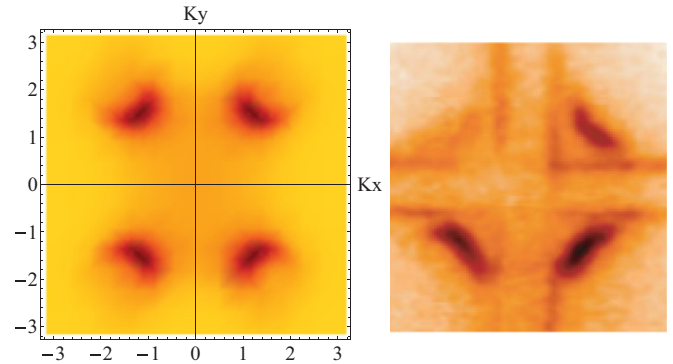

FIG. 3. (Color online) ARPES momentum-distribution map of the impurity-band (left panel), Eq. (5), with $(a_{im}/a)^2 = 0.4$, $t' = 0.7t$, and $\gamma = 0.94t$. Right panel: the experimental map of the Fermi surface in YBCO6.5 (Ref. [9]) (here $a = 1$).

dispersion, Eq. (3), holds for the whole Brillouin zone as long as we do not expand the valence-band energy operator $E(-i\overrightarrow{\nabla})$ to any finite order in $\overrightarrow{\nabla}$. The envelope function Eq. (1), works correctly to any power in k as long as the extension of the valence-band Wannier orbitals is much less than the extension of the impurity-band orbitals, $a_0 \ll a_{im} \approx a$.

One can parametrize the impurity-band dispersion by keeping nearest, t, and next-nearest, t', hopping integrals in Eq. (3). Thus $E_{im}^h(\mathbf{k}) = -2t\cos(k_y a) - 2t'[\cos(2k_x a) + \cos(2k_y a)]$ for holes with the lower band edge at the Γ point, which is compatible with the LDA + U band structure of YBCO6.0.[4] Every extra oxygen donates two holes, so that the impurity band is almost full with holes in YBCO6.5. Remaining holes partly reside in the CuO chains with a metalliclike one-dimensional Fermi surface detected in ARPES, and partly bound into in-plane preformed pairs (bipolarons) accounting for superconductivity.[18,19,21] The electron impurity-band dispersion,

$$E_{im}^e(\mathbf{k}) = 2t\cos(k_y a) + 2t'[\cos(2k_x a) + \cos(2k_y a)], \quad (4)$$

has its minima at the boundary of the reduced Brillouin zone, $\mathbf{k}^\star = (\pm\pi/2a, \pm[\pi - \cos^{-1}(t/2t')]/a)$, accounting for small electron pockets in MQO,[3] as seen in Fig. 2. Placing the Fermi level near the bottom of the electron impurity band $\mu = -2.5t$ yields the size of the electron Fermi pocket about 2% of the Brillouin zone as observed.[3] There is some anisotropy in the effective electron mass in the pocket, $m_x = \hbar^2/8t'a^2$ and $m_y = \hbar^2/(8t' - 3t^2/t')a^2$. Taking $m_x = 2m_e$ (Ref. [3]) and $t' = 0.7t$ provides a reasonable estimate for $t' \approx 32$ meV and $t \approx 46$ meV.

A momentum-distribution map of the impurity-band spectral function at the Fermi surface, $A(\mathbf{k},0) \propto 1/[(E_{im}^e(\mathbf{k}) - \mu)^2 + \gamma^2]$, is shown in Fig. 2 with the inverse quasiparticle lifetime $\gamma = 0.04t$ about the Dingle temperature measured in MQO experiments.[3] It hardly resembles the observed ARPES map,[9] which is not surprising because the impurity-band ARPES matrix element $M(\mathbf{K})$ strongly depends on the photoelectron momentum $\mathbf{K}$.[18] Calculating $M(\mathbf{K}) \propto \int d\mathbf{r} \exp(i\mathbf{K} \cdot \mathbf{r})\psi(\mathbf{r})$ with the impurity-band wave function, one obtains $M(\mathbf{K}) \propto f_{\mathbf{K}_\parallel}$, where $f_\mathbf{k}$ is the Fourier component of the impurity-band Wannier orbital, $f(\overrightarrow{\rho})$, introduced in Eq. (2).

The extension of this orbital is comparable to the lattice constant, which explains the strong dependence of the matrix element on the in-plane photoelectron momentum $\mathbf{K}_\parallel$.

Approximating $f(\overrightarrow{\rho})$ as the 2D Coulomb bound state $f_{im}(\rho)$ yields $M(\mathbf{K}) \propto 1/[1 + (K_\parallel a_{im})^2]^{3/2}$, and the ARPES momentum-distribution map of the Fermi surface, $I(\mathbf{K},0) \propto M(\mathbf{K})^2 A(\mathbf{K},0)$, is

$$I(\mathbf{K},0) \propto \frac{1}{[1 + (K_\parallel a_{im})^2]^3 [(E_{im}^e(\mathbf{K}_\parallel) - \mu)^2 + \gamma^2]}. \quad (5)$$

A very close resemblance between theoretical [Eq. (5)] and experimental ARPES maps is shown in Fig. 3. The theory reproduces the locations, relative intensities, and half-moon shape of the ARPES spots in YBCO6.5, reconciling puzzling ARPES and MQO data. In fact, the small electron pockets observed in MQO experiments[3] are seen in ARPES,[9] partially shadowed by the matrix element. The ARPES quasiparticle lifetime turns out much shorter than in MQO, presumably due to an instrumental broadening and a high level of impurity scattering off deposited potassium atoms on cleaved YBCO.[9] The ordering of excess oxygen ions in YBCO6.5 is essential for MQO. A significant departure from this particular doping in both directions should dampen the oscillations because of the increasing Dingle temperature, as observed.[3] In the electron-doped cuprates, one should expect an impurity band somewhat below the conduction band, if these compounds are doped charge-transfer insulators as the hole-doped ones. Then the outlined scenario with reversed holes and electrons also accounts for the small *hole* pockets observed in MQO of the *electron*-doped cuprates.[7] While there are no chains in $Nd_{2-x}Ce_xCuO_4$, the observation of MQO in the vicinity of the particular doping level $x \approx 0.165$ points to an ordered superstructure of Ce ions at their atomic density 1/6 providing the coherent impurity band.

[*]On leave from the Department of Physics, Loughborough University, Loughborough LE11 3TU, United Kingdom.

[1] A. Damascelli, Z. Hussain, and Zhi-Xun Shen, Rev. Mod. Phys. **75**, 473 (2003).

[2] N. E. Hussey, M. Abdel-Jawad, A. Carrington, A. P. Mackenzie, and L. Balicas, Nature (London) **425**, 814 (2003); M. Plate, J. D. F. Mottershead, I. S. Elfimov, D. C. Peets, R. Liang, D. A. Bonn, W. N. Hardy, S. Chiuzbaian, M. Falub, M. Shi, L. Patthey, and A. Damascelli, Phys. Rev. Lett. **95**, 077001 (2005); B. Vignolle, A. Carrington, R. A. Cooper, M. M. J. French, A. P. Mackenzie, C. Jaudet, D. Vignolles, Cyril Proust, and N. E. Hussey, Nature (London) **455**, 952 (2008).

[3] N. Doiron-Leyraud, C. Proust, D. LeBoeuf, J. Levallois, J. B. Bonnemaison, R. Liang, D. A. Bonn, W. N. Hardy, and L. Taillefer, Nature (London) **447**, 565 (2007); A. F. Bangura, J. D. Fletcher, A. Carrington, J. Levallois, M. Nardone, B. Vignolle, P. J. Heard, N. Doiron-Leyraud, D. LeBoeuf, L. Taillefer, S. Adachi, C. Proust, and N. E. Hussey, Phys. Rev. Lett. **100**, 047004 (2008); E. A. Yelland, J. Singleton, C. H. Mielke, N. Harrison, F. F. Balakirev, B. Dabrowski, and J. R. Cooper, *ibid.* **100**, 047003 (2008).

[4] I. S. Elfimov, G. A. Sawatzky, and A. Damascelli, Phys. Rev. B **77**, 060504(R) (2008), and references therein.

[5] A. S. Alexandrov, J. Phys. Condens. Matter **20**, 192202 (2008).

[6] B. J. Ramshaw, B. Vignolle, J. Day, R. Liang, W. N. Hardy, C. Proust, and D. A. Bonn, Nat. Phys. **7**, 234 (2011).

[7] T. Helm, M. V. Kartsovnik, M. Bartkowiak, N. Bittner, M. Lambacher, A. Erb, J. Wosnitza, and R. Gross, Phys. Rev. Lett. **103**, 157002 (2009).

[8] M. V. Kartsovnik, T. Helm, C. Putzke, F. Wolff-Fabris, I. Sheikin, S. Lepault, C. Proust, D. Vignolles, N. Bittner, W. Biberacher, A. Erb, J. Wosnitza, and R. Gross, New J. Phys. **13**, 015001 (2011).

[9] M. A. Hossain, J. D. F. Mottershead, D. Fournier, A. Bostwick, J. L. McChesney, E. Rotenberg, R. Liang, W. N. Hardy, G. A. Sawatzky, I. S. Elfimov, D. A. Bonn, and A. Damascelli, Nat. Phys. **4**, 527 (2008).

[10] V. I. Anisimov, J. Zaanen, and O. K. Andersen, Phys. Rev. B **44**, 943 (1991).

[11] M. M. Korshunov, V. A. Gavrichkov, and S. G. Ovchinnikov, I. A. Nekrasov, Z. V. Pchelkina, and V. I. Anisimov, Phys. Rev. B **72**, 165104 (2005).

[12] T. Das, R. S. Markiewicz, and A. Bansil, Phys. Rev. B **81**, 174504 (2010).

[13] S. G. Ovchinnikov, personal communication (2011).

[14] D. Fournier, G. Levy, Y. Pennec, J. L. McChesney, A. Bostwick, E. Rotenberg, R. Liang, W. N. Hardy, D. A. Bonn, I. S. Elfimov, and A. Damascelli, Nat. Phys. **6**, 905 (2010).

[15] I. Bozovic, G. Logvenov, M. A. J. Verhoeven, P. Caputo, E. Goldobin, and T. H. Geballe, Nature (London) **422**, 873 (2003).

[16] V. N. Denisov, C. Taliani, A. G. Malshukov, V. M. Burlakov, E. Schonherr, and G. Ruani, Phys. Rev. B **48**, 16714 (1993).

[17] G. Yu, C. H. Lee, D. Mihailovic, A. J. Heeger, C. Fincher, N. Herron, and E. M. McCarron, Phys. Rev. B **48**, 7545 (1993).

[18] A. S. Alexandrov and K. Reynolds, Phys. Rev. B **76**, 132506 (2007).

[19] A. S. Alexandrov and J. Beanland, Phys. Rev. Lett. **104**, 026401 (2010).

[20] S. C. Riggs, O. Vafek, J. B. Kemper, J. B. Betts, A. Migliori, F. F. Balakirev, W. N. Hardy, R. Liang, D. A. Bonn, and G. S. Boebinger, Nat. Phys. **7**, 332 (2011).

[21] A. S. Alexandrov, *Theory of Superconductivity: From Weak To Strong Coupling* (IOP, Bristol, 2003).

[22] M. B. Silva Neto, J. Phys. Condens. Matter **23**, 365601 (2011).

[23] E. Bascones, T. M. Rice, A. O. Shorikov, A. V. Lukoyanov, and V. I. Anisimov, Phys. Rev. B **71**, 012505 (2005).

[24] Z. Zhai, P. V. Parimi, J. B. Sokoloff, S. Sridhar, and A. Erb, Phys. Rev. B **63**, 092508 (2001).

[25] A. Behrooz and A. Zettl, Solid State Commun. **70**, 1059 (1989).

[26] R. Peierls, Z. Phys. **80**, 763 (1933).